NANOSCALE MECHANICS

A.N. CLELAND[(1)] AND M.L. ROUKES[(2)]

[(1)] *Department of Physics, University of California, Santa Barbara CA 93106*
[(2)]*Condensed Matter Physics 114-36, California Institute of Technology, Pasadena CA 91125*

Mechanically active single-crystal structures can now be fabricated with size scales of less than 100 nm in all three dimensions. These engineered structures have fundamental mechanical resonance frequencies approaching 1 GHz, with very little mechanical dissipation. Using such structures, we are developing a new class of devices with applications in electrometry, magnetometry, surface physics, and investigations of the physics of phonon-mediated processes. The methods used to fabricate these devices, combining electron-beam lithography and high precision etching, have been applied mostly to single-crystal Si and III-V substrates, but extension to other material systems is being pursued. In addition to practical applications, there exists the possibility of investigating fundamental quantum mechanical processes such as macroscopic quantum tunneling, in a *mechanical* system. In this report we describe our approaches to this topic.

1 Introduction

The application of nanometer scale patterning technology to the fabrication of mechanical structures is just beginning to be explored, as a natural extension of semiconductor micromachining and its related burgeoning commercial usage. We have developed a range of technical tools with which to fabricate mechanically suspended and mechanically active structures with size scales of less than 100 nm and mechanical response frequencies approaching 1 GHz. We envision a range of applications for this new technology, ranging from sensors to investigations of fundamental physics, such as phonon transport and macroscopic quantum tunneling.

2 Fabrication principles

We have fabricated devices from bulk *Si* substrates[1] and from *SIMOX* substrates, which include a 400 nm thick buried SiO_2 layer with a 200 nm thick top layer of single-crystal *Si*, as well as from *GaAs* heterostructures, including an *AlGaAs* sacrificial layer[2]. Lithographic processing was typically performed in four steps, consisting of an optically defined alignment layer, an scanning electron microscope (SEM) lithographically defined wiring layer, a contact pad definition layer, and an SEM-defined metal masking layer for anisotropic etching of the substrate. Following the anisotropic etch, a wet etch was used to remove the exposed regions of the sacrificial layer, which resulted in mechanical suspension of the structures. A schematic view of the processing steps is shown in Figure 1. In

Fig. 1(a), the unetched structure including metallized leads and metal mask is shown in cross-section. In Fig. 1(b), the structure following the anisotropic etch is shown, and in Fig. 1(c) the structure is shown following removal of the metal mask. Finally, in Fig. 1(d) we show the completed suspended structure.

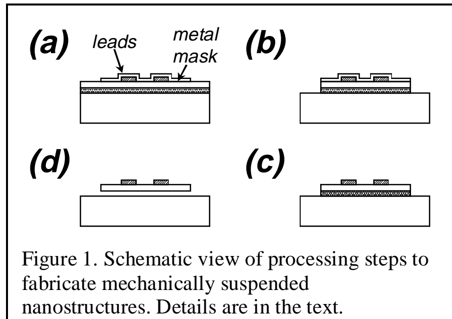

Figure 1. Schematic view of processing steps to fabricate mechanically suspended nanostructures. Details are in the text.

Using the technique described above, we have fabricated a number of suspended structures and have measured their mechanical resonance properties at a temperature of 4.2 K. An SEM micrograph of a cradle resonator is shown in Fig. 2(a), where the central beam has dimensions 7.8 μm×0.5 μm×0.2 μm. Other structures are shown in Fig. 2(b)-(d). The mechanical resonance frequencies for these structures range from a few MHz up to nearly 1 GHz for the shortest flexural resonator in Fig. 2(d).

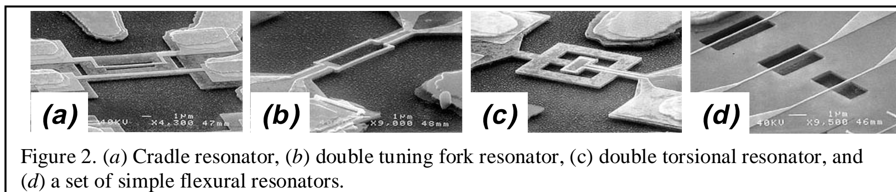

Figure 2. (a) Cradle resonator, (b) double tuning fork resonator, (c) double torsional resonator, and (d) a set of simple flexural resonators.

3 Measurement of mechanical properties

We measure the mechanical properties of these structures using a *magnetomotive* technique[1,3]. These measurements are made by placing the resonant structure in a transverse magnetic field. An alternating current is then applied through a metal electrode on the resonator surface, which drives the resonator by way of the Lorentz force, and the resulting motion of the resonator through the magnetic field generates an electromotive force that is detected by the measurement circuitry. The calculated resonance frequencies for these structures usually agree with the measured frequencies to within about 10%, roughly within the precision of our knowledge of the resonator's physical dimensions.

We have measured the resonance properties of cradle resonators, a number of simply suspended beams, torsional oscillators and tuning fork resonators (see Figure 2). The resonance curves for the cradle resonator and for the two tines of the tuning fork in Figure 3.

We have measured a fundamental resonance frequency for a simple beam at 110 MHz, and have fabricated structures with calculated resonance frequencies up

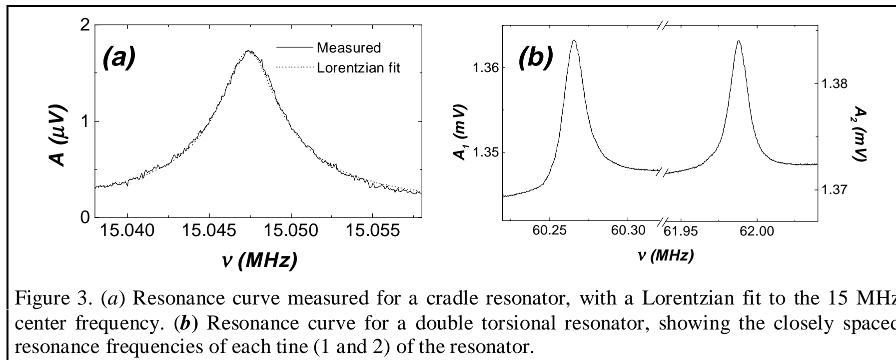

Figure 3. (*a*) Resonance curve measured for a cradle resonator, with a Lorentzian fit to the 15 MHz center frequency. (***b***) Resonance curve for a double torsional resonator, showing the closely spaced resonance frequencies of each tine (1 and 2) of the resonator.

to 800 MHz. The typical quality factors that we have measured range from 0.5-2×10^4, and are probably limited by losses in the support structure and the metallization layers. Measurements on the higher frequency resonators are in progress, and we are studying methods to increase the quality factors of our structures.

4 Electrometry

Elsewhere[4] we have described the fabrication and performance of a nanoscale mechanical electrometer, with a demonstrated charge sensitivity of 10^{-1} $e/\sqrt{\text{Hz}}$, exceeding that of state-of-the-art semiconductor devices. A thermal noise analysis indicates that such mechanical electrometers should ultimately reach sensitivities of order 10^{-6} $e/\sqrt{\text{Hz}}$, making them competitive with the cryogenic single-electron transistor[5], but with important added advantages such as higher temperature operation and response over greatly increased bandwidth.

An electron micrograph of our nanomechanical electrometer is shown in Figure 4. It is comprised of three principal components: electrodes, which experience an attractive force when a small charge is applied; a compliant mechanical element that moves in response to this force; and a displacement detector that provides a sensitive means of monitoring the charge-induced motion. In our experiments the compliant mechanical element forms a double torsional resonator, which, when deflected, returns to its rest position with a torsional spring constant G_0 and moment I. Its fundamental torsional resonance frequency is ω_o, and the mechanical loss is parameterized by a quality factor $Q = \omega_0/\Delta\omega$, where $\Delta\omega$ is the frequency width of the resonant response at half maximum.

The device includes an electrode for coupling charge, and two to monitor the mechanical displacement of the structure. One displacement-sensing electrode is in the form of a metal loop tracing the inner paddle's outer boundary, while the opposing charge-coupling gate electrode is fixed to the stationary substrate, at a distance d from the paddle. The mutual capacitance between these electrodes is represented by the parameter C. To measure a small charge, the gate electrode is biased by a charge q_0, which yields an electrostatic force $F_E = q_0^2/Cd$. Small

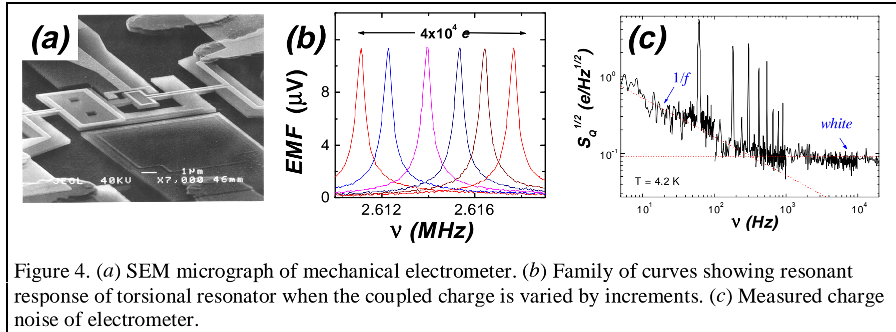

Figure 4. (*a*) SEM micrograph of mechanical electrometer. (*b*) Family of curves showing resonant response of torsional resonator when the coupled charge is varied by increments. (*c*) Measured charge noise of electrometer.

changes in the charge, δq, about the bias point q_0 alter the force by an amount $f_E = 2\,\delta q E_0$, where E_0 is the equilibrium electric field. This results in an effective torsional spring constant $G_{\rm eff} = G_0 + g$, where $g = -r\partial f_\theta/\partial\theta = -2r\delta q\partial E_0/\partial\theta$ (θ is the paddle torsion angle, E_θ the field component along the unit vector θ, and r the paddle radial dimension), and gives rise to a shift from the unperturbed resonance frequency, $\delta\omega/\omega_0 = g/2G_0$.

To perform electrometry we monitor the change in the resonance frequency due to the charge modulation of $G_{\rm eff}$. This approach can be especially sensitive if the quality factor of the resonator is high. In Figure 4(*b*) we show the amplitude of the EMF measured as a function of drive current frequency, with fixed current amplitude. Each trace was taken with a different amount of dc voltage applied to the gate electrode. The range of voltages applied corresponds to a total change in the coupled charge of about 4×10^4 *e*.

We have measured the spectral density of the charge noise, $S_Q(\nu)$, which limits the sensitivity of this device, shown in Figure 4(*c*).The charge noise is dominated by $1/f$ noise at low frequencies, with a noise level of $S_Q^{1/2} = 0.6\ e/\sqrt{\rm Hz}$ at $\nu = 10$ Hz. Above a frequency of about 500 Hz the noise levels out to a white noise floor of $S_Q^{1/2} = 0.09\ e/\sqrt{\rm Hz}$. This level of charge noise is competitive with state-of-the-art electrometers based on cryogenically-cooled field-effect transistors[6].

We can estimate the thermal limit to the charge sensitivity. With a drive amplitude of 30 mrad and a first-stage amplifier noise temperature of 300 K (roughly the value in the experiment), a voltage bias of 10 V on the gate gives a thermally limited charge noise of $7\times10^{-4}\ e/\sqrt{\rm Hz}$. A state-of-the-art cryogenic amplifier, with a noise temperature of 10 K, would reduce this value to 1×10^{-4}

$e/\sqrt{\text{Hz}}$. This is comparable to a SET operating at 50 mK and measured at 1 kHz, which is limited by $1/f$ processes[5]. If we reduce the torsional rod cross-section while increasing its length, so that each rod has dimensions $0.1\times0.1\times2$ μm^3, and the paddle dimensions are reduced to $0.1\times0.5\times1$ μm^3 (the last dimension the paddle radius r), we obtain a resonance frequency $\nu_0 = 7$ MHz. Placing the gate electrode 0.1 μm from the paddle edge, we obtain a charge noise floor of $\sim3\times10^{-6}$ $e/\sqrt{\text{Hz}}$, an improvement of nearly two orders of magnitude.

These first experiments clearly show that the nanometer-scale mechanical electrometer provides a new means for ultrasensitive charge measurement. These devices are unique in that they offer a much higher potential bandwidth than the SET. A further advantage of the mechanical electrometer is its ability to operate at 4.2 K (or higher), as compared to millikelvin temperatures required for very low noise SETs. This opens real possibilities for useful applications such as single-photon photodetection[7] or ultrasensitive scanned electrometry[8].

5 Macroscopic quantum tunneling

We now turn to a variation on the use of the electric forces applied to mechanical devices, and focus our attention upon a bistable mechanical system consisting of an elastic cantilevered beam displaced by a strongly inhomogeneous electric field, an idealization of the mechanical electrometer described above. We place a charged, mechanically rigid base electrode near the small oppositely-charged mechanical resonator, as shown in Figure 5. The resulting electrostatic force then depends strongly upon the position of the resonator. Assuming that the electrodes are small compared to the electrode–resonator spacing δ, we may approximate the electrostatic force as $F_E=\alpha q^2/(16\pi\varepsilon_0\delta^2)$, where q is the (assumed constant) charge on the resonator and the constant α, of order unity, is a correction due to the nonzero dimensions of the electrodes. We assume the elastic restoring force F_R of the resonator is linear with spring constant k_s and rest point δ_0, so that $F_R = k_s(\delta-\delta_0)$. Parameterizing the system with dimensionless position $y = \delta/\delta_0$, energy $E_0 = k_s\delta_0^2/2$, and coupling parameter $z = \alpha q^2/16\pi\varepsilon_0 k_s\delta_0^3$, we define the potential function $u(y)$ as $u(y) = -(1/E_0)\int(F_E+F_R)dy = -2z/y+(y-1)^2$.

A metastable minimum exists for values of z such that $0 \le z < z_C = 4/27$. For operating conditions which place the resonator within this metastable minimum, the resonator executes small oscillations with dimensionless frequency

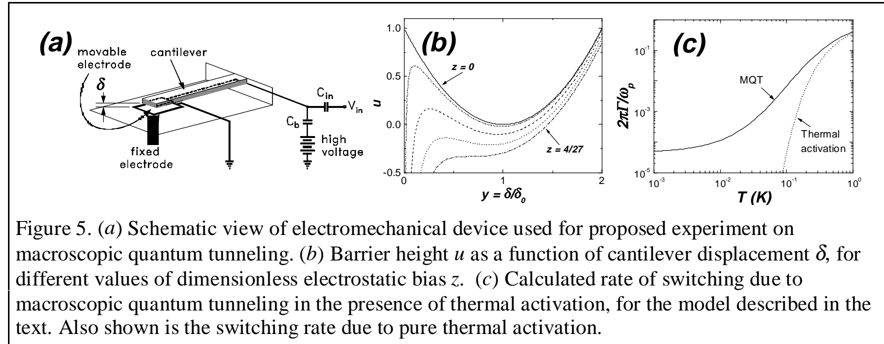

Figure 5. (a) Schematic view of electromechanical device used for proposed experiment on macroscopic quantum tunneling. (b) Barrier height u as a function of cantilever displacement δ, for different values of dimensionless electrostatic bias z. (c) Calculated rate of switching due to macroscopic quantum tunneling in the presence of thermal activation, for the model described in the text. Also shown is the switching rate due to pure thermal activation.

$\Omega = \omega_{res}/\omega_0 = (1-2z/y_{min}{}^3)^{1/2}$. Here ω_0 is the resonant frequency in the absence of a charge bias on the electrodes. For a cantilever of dimensions $L \times w \times t$, Young's modulus E, and mass density ρ, the resonance frequency is $\omega_0/2\pi = 0.16(E/\rho)^{1/2} t/L^2$, the mass is $m = \rho wLt$, and the spring constant is $k_s = \beta\omega_0{}^2 m$. Here β is a constant of order unity determined by the distribution of the force F_E; we set $\beta = 1$.

Let us consider preparing the system in equilibrium with $z = 0$, hence $y = 1$. Then, by adiabatically increasing the charge bias, we gradually reposition the resonator within the (new) potential minimum. The minimum energy resting point $y_{\min}$ is thereby changed, and the barrier height Δu and resonant frequency Ω are reduced from their maximum values to zero as the coupling z is increased to z_c. A plot of this dependence is shown in Fig. 5(b).

This device has two stable states, one in which the resonator is in contact with the fixed counterelectrode (the "pulled-in" state) and the other where it rests within the metastable potential minimum. If we permit charge transferal to occur when the resonator contacts the base electrode, the equilibrium potential function will reset to zero charge bias as the charge disperses.

The two-state nature of this device is similar to that of the underdamped Josephson junction, which switches from the zero- to the finite-voltage state as the current bias is increased[9]. It is thus natural to consider how the present system might exhibit thermal activation, resonant activation and macroscopic quantum tunneling at low temperatures near z_C, the critical charge bias. Especially appealing here is that the extremely high quality factors of single-crystal resonators allow new tests of the theory of thermal activation[10] from the metastable state. To our knowledge thorough and explicit tests of these theories in the high Q limit have yet to be performed, as experiments performed using Josephson junctions[11] merely showed *consistency* with theory.

Kramers' theory[10] elucidates different physical regimes of thermal activation, delineated by the degree of damping. Given a barrier height E_b, the activation rate is $\Gamma_{th} = a_t(\omega_{res}/2\pi)exp(-E_b/k_BT)$, where in the moderately damped limit the prefactor $a_t = 1$, while in the limit of small damping $Q >> 2\pi E_b/k_BT$ the prefactor has the form $a_t = 2\pi E_b/k_BTQ$. A careful measurement of this prefactor would be of great interest, and given that the quality factor of an electromechanical resonator can be varied *in situ*[12], it is plausible that this weak prefactor could be separated from the dominant exponential term.

Rigorous measurements of the rate of macroscopic quantum tunneling (MQT) from a metastable minimum have been performed with Josephson tunnel junctions[13] as well as with the rf SQUID[14]. The electromechanical device described here provides a new system in which analogous measurements can be made. Here, as in the case of thermal activation, studies become possible for the first time in an unexplored regime of extremely low damping. Using the WKB approximation[15] for tunneling into a continuum of states, one can estimate the rate of tunneling for this system. This tunneling rate, in the limit of zero damping, has the form $\Gamma_Q = a_q(\omega_{res}/2\pi)exp\{-4(E_0/\hbar\omega_{res})b_0\}$, where $a_q \approx (120\pi(4E_0/\hbar\omega_{res})b_0)^{1/2}$. The term b_0 is the dimensionless WKB integral for tunneling under the potential barrier.

The crossover from thermal activation to quantum tunneling occurs at a temperature[16] $k_BT_{cr} = \hbar\omega_{res}/2\pi$, so a fundamental resonance frequency above 10^9 Hz is desirable. A reasonable tunneling exponent could be achieved with a cantilevered Si beam with dimensions $30\times1\times1$ nm^3, with a resonator-electrode spacing of 1 nm. Making the rough assumption that the bulk mechanical constants of Si hold for such a small structure, we use $E_{100} = 1.33\times10^{11}$ N/m^2 and $\rho = 2330$ kg/m^3, so the unbiased resonant frequency would be about 12 GHz. Reasonable tunnel rates could be achieved for values of z within about 1% of z_c, corresponding to an electrode charge bias of $q \approx 0.57\ e$, approximating the factor $\alpha = 1$; this corresponds to a bias voltage of order 0.1 V. While theories of MQT do not display a functional change in the high-Q limit, a measurement of the *linewidths* of the bound states in the metastable minimum would be of great interest, as they probe the dissipation function at high frequencies about ω_{res}[17], and could be performed in a manner similar to that used in the Josephson junction[18] and the rf SQUID[19].

6 Summary

We have described the fabrication and measurement techniques we use to create and characterize nanometer-scale mechanical resonators, with minimum size scales of 100 nm and mechanical resonance frequencies approaching 1 GHz. We have described some applications of these devices, as electrometers, and as a potential tool for investigating macroscopic quantum tunneling in a mechanical

structure. This is a new field of research and we anticipate a wide range of potential applications.

7 References

[1] A.N. Cleland and M.L. Roukes, "Fabrication of nanoscale mechanical structures from bulk Si crystals", *Appl. Phys. Lett.* **69**, 2653 (1996).

[2] T.S. Tighe, J.M. Worlock, M.L. Roukes, "Direct thermal conductance measurements on suspended monocrystalline nanostructures", *Appl. Phys. Lett.* **70**, 2687 (1997).

[3] D.S. Greywall *et al.*, *Phys. Rev. Lett.* **72**, 2992 (1994); D.S. Greywall, B. Yurke, P.A. Busch, S. Arney, *Europhys. Lett.* **34**, 37 (1996).

[4] A.N. Cleland and M.L. Roukes, "Nanostructure-based mechanical electrometry", *Nature* **392**, 160 (1998).

[5] G. Zimmerli, T.M. Eiles, R.L. Kautz, J.M. Martinis, "Noise in the Coulomb blockade electrometer", *Appl. Phys. Lett.* **61**, 237-239 (1992).

[6] F. Bordoni, G. Maggi, A. Ottaviano, G.V. Pallotino, "Very low noise cooled audiofrequency preamplifier for gravitational research", *Rev. Sci. Inst.* **52**, 1079 (1981).

[7] A.N. Cleland, D. Esteve, C. Urbina, M.H. Devoret, "Very low noise photodetector based on the single electron transistor", *Appl. Phys. Lett.* **61**, 2820 (1992).

[8] M.J. Yoo, T.A. Fulton, H.F. Hess, R.L. Willett, L.N. Dunkleberger, R.J. Chichester, L.N. Pfeiffer, K.W. West, *Science* **276**, 579-582 (1997).

[9] T.A. Dolan and L.N. Dunkleberger, *Phys. Rev. B* **9**, 4760 (1974).

[10] V.I. Melnikov, *Phys. Reports* **209**, 1 (1991) and references therein; H.A. Kramers, *Physica* **7**, 285 (1940)

[11] P. Silvestrini, O. Liengme and K.E. Gray, *Phys. Rev. B* **37**, 1525 (1988); P. Silvestrini *et al.*, *Phys. Rev. Lett.* **60**, 844 (1988); P. Silvestrini and B. Ruggiero, *Nuov. Cim. D* **14**, 555 (1992).

[12] A.N. Cleland and M.L. Roukes, "External control of dissipation in radiofrequency mechanical resonators", *to be published in Sensors and Actuators* (1998).

[13] R.F. Voss and R.A. Webb, *Phys. Rev. Lett.* **47**, 265 (1981); M.H. Devoret, J.M. Martinis, J. Clarke, *Phys. Rev. Lett.* **55**, 1908 (1985).

[14] D.B. Schwartz, B. Sen, C.N. Archie, J.E. Lukens, *Phys. Rev. Lett.* **55**, 1547 (1985); *Phys. Rev. Lett.* **57**, 266 (1986).

[15] A.O. Caldeira and A.J. Leggett, *Ann. Phys. (N.Y.)* **149**, 374 (1983).

[16] I. Affleck, *Phys. Rev. Lett.* **46**, 388 (1981).

[17] C. Urbina, D. Esteve, J.M. Martinis, E. Turlot, M.H. Devoret, H. Grabert, S. Linkwitz, *Physica B* **169**, 26 (1991); H. Grabert, P. Olschowski and U. Weiss, *Phys. Rev. B* **36**, 1931 (1987).

[18] J.M. Martinis, M.H. Devoret, J. Clarke, *Phys. Rev. Lett.* **55**, 1543 (1985).

[19] R. Rouse, S. Han and J.E. Lukens, *Phys. Rev. Lett.* **75**, 1614 (1995).